Journal of Environmental Health Science and Engineering
https://doi.org/10.1007/s40201-019-00347-0

RESEARCH ARTICLE

Atenolol adsorption onto multi-walled carbon nanotubes modified by NaOCl and ultrasonic treatment; kinetic, isotherm, thermodynamic, and artificial neural network modeling

Bahare Dehdashti[1,2] · Mohammad Mehdi Amin[2,3] · Abdolmajid Gholizadeh[4] · Mohammad Miri[5] · Lida Rafati[6]

Received: 28 August 2018 / Accepted: 23 January 2019

Abstract

The removal of pharmaceutical pollutants from the aqueous environment is a great environmental concern, mainly due to their diversity, high consumption, and sustainability. In the current study, we aimed to investigate the ability of multi-walled carbon nanotubes (MWCNTs) modified by sodium hypochlorite (NaOCl) and ultrasonic treatment in refining wastewaters contaminated with Atenolol β-blocker drug (ATN). The physical and structural characteristics of the raw MWCNTs and modified MWCNTs (M-MWCNTs) were analyzed using SEM, TEM, Raman spectroscopy, TGA, and FT-IR techniques. The effects of different parameters, including pH, initial concentration, contact time, and temperature were studied and optimized. Subsequently, the adsorption data were analyzed by several kinetic and equilibrium isotherm equations and modeled by artificial neural network (ANN). Highest ATN removal (87.89%) (($q_{e,exp}$ = 46.03 mg g^{-1})) occurred on the adsorbent activated within 10 s of ultrasonication time and NaOCl 30%. Moreover, adsorbent modification significantly improved the ATN removal, so that the removal rate on the raw MWCNTs was about 58%, but in the same conditions, M-MWCNTs removed more than 92% of the adsorbate. The adsorption process reached equilibrium after 90 min under the optimized pH of 6. According to ANN modeling, approximately the whole values dispersed around the 45°line, indicating a good compatibility between the trial results and ANN-predicted data. The modification of MWCNTs in proper ultrasonic power via appropriate concentration of NaOCl solution removed many of the impurities and significantly improved the adsorption performance of MWCNTs.

Keywords Atenolol · Wastewater · Multi-walled carbon nanotube · Artificial neural network

Introduction

Recently, the use of pharmaceutical compositions has dramatically grown in human beings and animals, but due to diversity, high consumption, and sustainability, they are one of the most important water contaminants [1, 2]. Atenolol (ATN) is one of the most prescribed antagonist β-blocker drugs [3], widely used to treat cardiovascular diseases, reduce the probability of heart attacks, treat angina (chest pain) as well as hypertension, and control some forms of heart arrhythmias. Therefore, it extensively exists in hospital wastewaters [4, 5]. Maszkowska, et al. claimed that ATN could alter the amount of testosterone in human by generating disruption in endocrine glands [6].

Since the most consumed β-blockers are not fully metabolized in the human body, major parts of these drugs (about 90%) are excreted through urine as unaltered [7]. Lack of adequate and sufficient technologies has caused the necessary removal of these compounds from municipal and hospital

Electronic supplementary material The online version of this article (https://doi.org/10.1007/s40201-019-00347-0) contains supplementary material, which is available to authorized users.

✉ Abdolmajid Gholizadeh
gholizadeh_eng@yahoo.com; gholizadeh.a@esfrum.ac.ir

[1] Student Research Committee, School of Health, Isfahan University of Medical Sciences, Isfahan, Iran

[2] Department of Environmental Health Engineering, School of Health, Isfahan University of Medical Sciences, Isfahan, Iran

[3] Environment Research Center, Research Institute for Primordial Prevention of Non-communicable Disease, Isfahan University of Medical Sciences, Isfahan, Iran

[4] Esfarayen Faculty of Medical Sciences, Esfarayen, Iran

[5] Department of Environmental Health, School of Public Health, Sabzevar University of Medical Sciences, Sabzevar, Iran

[6] Deputy of Health, Hamadan University of Medical Sciences, Hamadan, Iran

Published online: 06 February 2019

wastewater treatment plants (WWTPs) ineffective. Consequently, ATN concentration in WWTP outputs can increase, ranging from about 0.78 mg L^{-1} to 6.6 mg L^{-1}, which is much more than the permissible level (10 ng L^{-1}) [8]. In a study, ATN, Metoprolol, and Propranolol were frequently detected in the WWTP effluents. In this study, the maximum concentrations of ATN in influents and effluents were 2.346 mg L^{-1} and 1.707 mg L^{-1}, respectively [9].

As previously mentioned, the conventional wastewater treatment processes, such as activated sludge, are not enough to remove ATN and other similar pharmaceutical compounds completely from the aqueous environment. So, complementary treatment methods such as advanced oxidation processes (AOPs) [10, 11], ozonation [12], and membrane filtration [5, 13] are often applied along with the conventional methods for treating the wastewater containing β-blockers. However, low mineralization and increased toxicity of wastewater, expensive equipment, and high-energy consumption are among the disadvantages attributed to some of these processes [7, 11, 14].

Recently, the adsorption process has been reported as an alternative for removing the persistent pollutants because of its ease of use, lower energy consumption, high efficiency, safety, and non- or less toxicity [7, 8, 15, 16]. Carbon nanotubes (CNTs) are unique macromolecules that have attracted a lot of attention due to their high thermal resistance, chemical stability, and fast operation [17]. These nanomaterials have the necessary chemical, mechanical, and electrical properties to be used in biosensors and electronic transistors [1]. Moreover, considering the porosity and hollow structure, functional groups at the surface, and hydrophobicity, CNTs can be used as an adsorbent in water purification [18, 19]. One of the main drawbacks of conventional adsorbents is their rapid saturation and low adsorption capacity [20]. Therefore, in the current study, we tried to investigate the adsorbent surface modification by sodium hypochlorite (NaOCl), and employing ultrasonic waves as new, inexpensive, and environmentally sound methods for refining the wastewaters containing ATN β-blocker drug [21]. Naghizadeh et al. (2017) reported that we can regenerate graphene nanoparticles with an ultrasonic process as 85.37% and 72.47% at frequencies of 60 kHz and 37 kHz, respectively. [22]. However, we assumed that the modification of adsorbent surface by using these methods could increase the efficiency of removal of pollen adsorbents.

Adsorption is a complex process, so describing it in the form of modeling systems such as artificial neural network (ANN), can help us in better understanding of the involved mechanisms [1]. Accordingly, the effects of different parameters such as pH, initial concentration of ATN, contact time, and temperature were studied and optimized. Subsequently, the adsorption data were analyzed by several kinetic and equilibrium isotherm equations and modeled by artificial neural network (ANN).

Material and methods

Instruments and reagents

All chemicals such as ATN (chemical formula = $C_{14}H_{22}N_2O_3$), NaOCl, HCl, and NaOH, etc. were purchased from Sigma Aldrich without further purification. Raw MWCNTs (Cheap Tubes Inc., USA) were used as the base adsorbent. The physical and chemical characteristics of selected adsorbent are listed in Table 1.

Modification of adsorbent

In order to modify the adsorbent surface, the raw MWCNTs were initially contacted with NaOCl solutions (30% and 60% purities), placed on a stirrer for 2 h at 300 rpm, and then dried. Subsequently, the pretreated MWCNTs were placed in an ultrasonic bath at a frequency of 22 kHz and different times (1, 5, 10, and 20 s). Next, they were rinsed and heated at 70 °C for 7 h in an oven, and kept in the desiccator for next uses.

Batch adsorption experiments

The experimental design of this study was one factor at a time. The affective factors on the adsorption process, including pH (3–10), contact time (2–150 min), initial concentration of ATN (2, 5, 7.5 and 10 mg L^{-1}), MWCNTs and M-MWCNTs doses (50, 75, 100, 125, 150 and 200 mg L^{-1}), and solution temperature (20–50 °C) were investigated and optimized in a laboratory scale. It should be noted the ATN solutions without any adsorbents, as well as the untreated adsorbents were used as controls. Accordingly, the ATN adsorption on the flask wall was negligible.

Measurements and data analyzing

The ATN concentrations in the aqueous phase were measured via a high-performance liquid chromatography (HPLC, CE4200, England). Samples were pre-filtered before using in the chromatographic studies by a 0.45 μm PTFE hydrophilic sterile filter. Meanwhile, the HPLC mobile phases were

Table 1 Physical and chemical properties of MWCNTs used during this study

Characteristics	Values
Purity	> 95%
Outer Diameter	< 8 nm
Inner Diameter	2–5 nm
Length	>10 μm
Specific Surface Area	> 500 m^2 g^{-1}
Electric Conductivity	>100 s cm^{-1}
Tap density	0.27 g cm^{-3}
True density	~2.1 g cm^{-3}

Acetonitrile (ratio of 55% to 100%) and 0.05 M Phosphate buffer (ratio of 45% to 0%), respectively, at 1.5 mL min^{-1} flow rate. The absorbances of the sample solutions were recorded at 224.20 nm.

Surface morphology, shape, as well as the size of MWCNTs and M-MWCNTs were investigated through scanning electron microscopy (SEM, Stereo Scan LEO, Model-400) and transmission electron microscopy (TEM, PHILIPS, EM400). SEM image of raw MWCNTs (Fig. 1) showed a uniform distribution and regular filamentous structure. Raman spectroscopy (Renishaw, RM 1000) technique was also applied to find the spectral fingerprint of materials. Furthermore, an FT-IR spectrometer (Bruker Optics, TENSOR 27) was used to determine the functional groups and formation of chemical bonds in MWCNTs and M-MWCNTs.

The ATN removal efficiency (E, %) and adsorption capacities (q, mg g^{-1}) of MWCNTs and M-MWCNTs were determined based on the following equations [23]:

$$E = \frac{(C_0 - C_e)}{C_0} \times 100 \quad (1)$$

$$q = \frac{V}{m} \times (C_0 - C_e) \quad (2)$$

C_o and C_e (mg L^{-1}) are the initial and equilibrium ATN concentrations, respectively. V (L) is solution volume, and m (g) is the mass of each adsorbent used.

Kinetics of adsorption

Kinetic equations are applied to explain the transport behavior of the adsorbate molecules on the adsorbent surface per time unit. In the current study, four kinetic models were used to define the adsorption kinetics. The non-linear forms of these models are presented below [24]:

$$\text{Pseudo first order} \quad q_t = q_e[1-\exp(-K_1 t)] \quad (3)$$

$$\text{Pseudo second order} \quad q_t = K_2 q_e^2 t/(1 + K_2 q_e t) \quad (4)$$

$$\text{Intra-particle diffusion} \quad q_t = K_p t^{0.5} \quad (5)$$

$$\text{Elovich} \quad q_t = \beta \text{Ln}\,(\alpha\beta t) \quad (6)$$

q_e and q_t (mg g^{-1}) are adsorption capacities of MWCNTs and M-MWCNTs at equilibrium and time t, respectively. The constants of K_1 (1 min^{-1}), K_2 (g mg^{-1} min^{-1}), and K_p (mg g^{-1} $min^{-1/2}$) are related to pseudo first order, pseudo second order, and intra-particle diffusion model, respectively. In addition, α (mg g^{-1} h^{-1}) and β (g mg^{-1}) are the constants of Elovich model.

Isotherm of adsorption

Equilibrium isotherms describe the relationship between adsorbate concentration and adsorbent capacity at a constant temperature. Here, Freundlich, Langmuir, and Temkin isotherms were employed to evaluate the experimental data. The non-linear expressions of used isotherm models are given in equations below [7, 25]:

$$\text{Lanumuir} \quad q_e = (q_m K_L C_e)/1 + K_L C_e \quad (7)$$

$$\text{Freundlich} \quad q_e = K_F C_e^{1/n} \quad (8)$$

$$\text{Temkin} \quad q_e = q_m \ln(K_T C_e) \quad (9)$$

The constants of K_L, K_F, and K_T are related to Langmuir, Freundlich, and Temkin models, respectively. Moreover, 1/n is the Freundlich constant associated to adsorption intensity, and q_m (mg g^{-1}) is the maximum theoretical adsorption capacity of adsorbent.

Furthermore, R_L that is a dimensionless separation factor in the Langmuir model was calculated as:

$$R_L = \frac{1}{1 + K_L C_0} \quad (10)$$

Thermodynamics of adsorption

Three main parameters, comprising the standard enthalpy (ΔH^o), standard entropy (ΔS^o), and free energy change (ΔG^o) were determined to study the adsorption thermodynamic. Often, Vant Hoff relation is used to show the relationship between temperature (T, °K) and adsorption equilibrium constant, ($K_c = q_e/C_e$), and is expressed as [16, 26]:

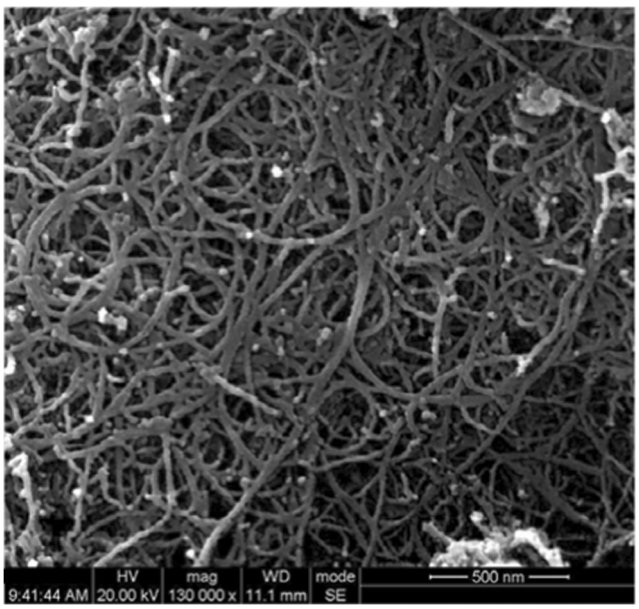

Fig. 1 scanning electron microscopy (SEM) image of raw MWCNTs

$$\mathrm{Lnk_c} = -\frac{\Delta H^{\circ}}{RT} + \frac{\Delta S^{\circ}}{R} = -\frac{\Delta G^{\circ}}{RT} \tag{11}$$

where T (°K) is the temperature of solution and R is the universal gas constant (8.314 J mol^{-1} K^{-1}). ΔH^{o} and ΔS^{o} are the slope and intercept of a linear diagram of Ln (q_e/c_e) versus 1/T, respectively. The value of ΔG^{o} can also be determined through the following equation:

$$\Delta G^{\circ} = -RTLnK_c \tag{12}$$

Validity of kinetic and isotherm models

Correlation coefficient (R^2), Chi-square (X^2) and normalized standard deviation (NSD) were used to assess the validity of kinetic and isotherm models. X^2 and NSD are defined as [27]:

$$X^2 = \sum_{i=1}^{n} \left[\frac{q_{i,exp} - q_{i,cal}}{q_{i,cal}} \right]^2 \tag{13}$$

$$\mathrm{NSD} = 100\sqrt{\frac{1}{N-1}\sum_{i=1}^{N}\left[\frac{q_{i,exp} - q_{i,cal}}{q_{i,exp}}\right]^2} \tag{14}$$

$q_{i,exp}$ and $q_{i,cal}$ (mg g^{-1}) are the experimental and calculated q of ATN adsorption at time t, and N is the number of measurements made. The R^2 values close to 1 as well as smaller X^2 and NSD values indicate more accurate estimation of q_t [28].

Modeling based on artificial neural network (ANN)

The Neural Network Toolbox in MATLAB R2012a was employed to model and predict the ATN adsorption efficiencies on adsorbents used. Here, a three-layer ANN consisting of hidden, input, and output layers was used. ANN model had a tangent sigmoid transfer function at the hidden layer, a linear transfer function at output layer, and Levenberg–Marquardt back propagation algorithm with 1000 iterations. The data obtained from the experiments, 70% for training and 30% for the testing set, were classified randomly into three categories, including three neurons (ATN concentration (mg L^{-1}), contact time (min), and M-MWCNTs dose (g)), one neuron (ATN removal percentage) in the output layer, and 1 to 25 neurons in the hidden layer. The data were then normalized between 0.1 and 0.9 to avoid computational problems. The following normalization equation was used for modeling:

$$y = \frac{x_i - x_{min}}{x_{max} - x_{min}} \times 0.8 + 0.1 \tag{15}$$

where y is the normalized value of x_i, and x_{max} and x_{min} are associated with the maximum and minimum values of x_i, respectively. Ultimately, the ANN removals were modeled according to the coefficient of determination (R^2) and mean squared error (MSE), which can be defined as:

$$\text{coefficient of determination}\left(R^2\right) = 1 - \frac{\sum_{i=1}^{N}\left(y_{p,i} - y_{exp,i}\right)}{\sum_{i=1}^{N}\left(y_{p,i} - y_{av}\right)} \tag{16}$$

$$\mathrm{MSE} = \frac{1}{N}\sum_{i=1}^{N}\left(\left|y_{p,i} - y_{exp,i}\right|\right)^2 \tag{17}$$

where $y_{p,i}$ is the predicted value of ANN model, $y_{exp,i}$ is the experimental value. N is the number of data, and y_{av} is the average of the experimental values.

Results and discussion

M-MWCNTs characteristics

Figure 2a-c indicates the TEM of MWCNTs treated via 30% NaOCl and in different ultrasonication time. Fig. 2a, b shows a tubular structure of M-MWCNTs, when they have not lost their structures yet. However, MWCNTs have been deformed in Fig. 2c, while isolated nanotubes still exist at the edges of bundles of aggregates.

The thermal stability of the M-MWCNTs has been depicted in Fig. 3. Based on the thermal gravimetric analysis (TGA); M-MWCNTs are stable without any significant damage from about 40 °C to 537.88 °C. However, they began to decay from 537.88 °C, continued to a temperature of about 620 °C, and after this point, no other weight loss was observed. In this temperature range, weight loss was 96.33%. This can be justified by the loss of organic matter and the water molecule adsorbed by M-MWCNTs [29]. The derivative thermogravimetric (DTG) analysis showed only one large digital interceptor at 582.17 °C.

Moreover, Raman's technique, which is a spectroscopy method based on the scattering phenomenon and is unique for each molecule, was used to find out the structure of a composite (Fig. 4). In the Raman spectrum of M-MWCNTs, two sharp peaks are seen; the D band (about 1340 cm^{-1}) was caused by the disordered structure and the G band, which is the first-order Raman band, appeared at about 1580 cm^{-1}. The G band that was higher than the D band is related to the in-plane vibrational mode of C-C group.

FT-IR spectra of MWCNTs and M-MWCNTs are also presented in Fig. 5. The MWCNTs spectrum shows the

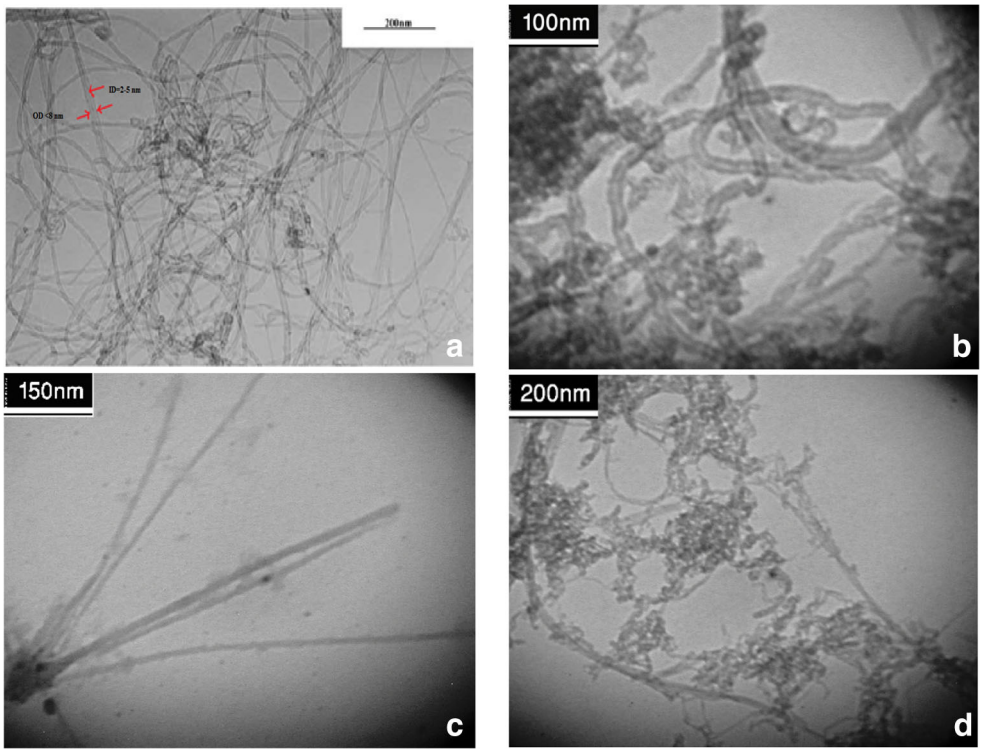

Fig. 2 TEM images of M-MWCNT (Ultrasonication time of a: untreated MWCNT, b: 5 s, c: 10 s, and d: 20 s. NaOCl concentration of 30%)

presence of various functional groups such as hydroxyl, carboxyl, and carbonyl in carbon nanotubes, but in M-MWCNTs, many of the impurities were removed. The dominant peaks at 1566 and 2352 cm^{-1} in M-MWCNTs are related to the stretching vibration characteristic of C=C and C-O groups, respectively. Furthermore, the peaks that appeared at 1708 and 1150 cm^{-1} are associated with the C=O group. These results are consistent with those obtained from Raman's spectroscopy.

The effect of variables

Ultrasonication

The effect of different ultrasonication time on the modification of MWCNTs is represented in Table 2. As shown, by increasing the ultrasonication time of MWCNTs from 1 to 5 and then to 10 s, the efficiency of ATN removal onto the adsorbent increased. The highest removal (87.89% ± 2.3) occurred in

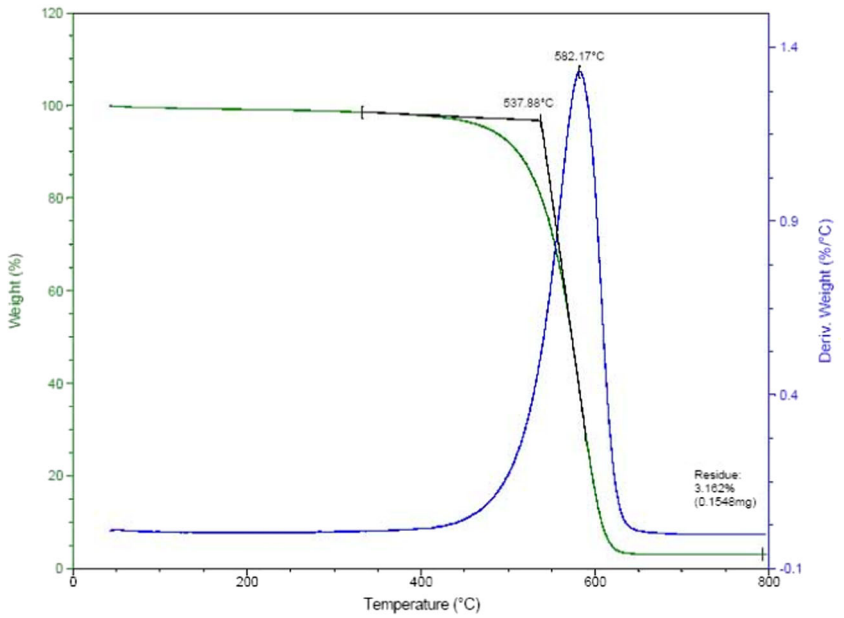

Fig. 3 TGA and DTG profiles of M-MWCNTs

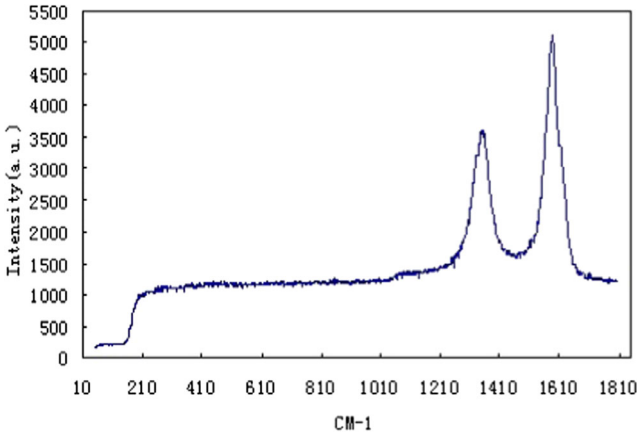

Fig. 4 Raman spectra of M-MWCNTs

the adsorbent activated within 10 s, but increasing the activation time to 20 s reduced the removal efficiency, which is likely because of structural damage. The surface ultrasonic treatment can remove catalyst particles, increase porosity, shorten the length of the nanotubes, and increase the specific surface area of CNTs [30, 31]. Furthermore, high performance, short duration, and environmental soundness are other benefits of the adsorbent ultrasonic modification [19]. Naghizadeh et al. (2017) regenerated as 85.37% and 72.47% of graphene nanoparticles with an ultrasonic process at pH of 11 during 60 min and frequencies of 60 kHz and 37 kHz, respectively, [22]. Similar results were obtained in the related literature. In a study by Omastova et al. (2014), CNTs were modified via anodic surfactants, and ultrasonication (64 or 360 W). Their results showed that the modification of MWCNTs in high ultrasonic power (>64 W) can reduce its electrical conductivity [32]. Also, Dotto et al. (2015) concluded modifying chitin surface by ultrasonic waves increases its active surface and porosity [33].

NaOCl pretreatment

In the case of NaOCl concentration, the solution having 30% concentration indicated better results and an increase in NaOCl concentration to 60% resulted in a significant reduction of the efficiency (Table 2). This finding can be justified by the fact that the balanced chlorine concentration of 30% increases the adsorbent porosity, which led to an improvement in the removal efficiency. Su et al. (2010) found that the untreated CNTs have more porosity in micropores but less porosity in mesopores as compared to the CNT(NaOCl) [34]. When the NaOCl solution of 60% is used, the increased chlorine oxidizes carbon nanotubes, and thereby, the electrical conductivity is reduced [35]. Yu et al. (2011) attributed the adsorption of toluene, ethylbenzene and xylene (TEX) on NaOCl-treated MWCNTs to the combined action of hydrophobic interaction, π-π bonding interaction between the aromatic ring of TEX and the oxygen-containing functional groups of MWCNTs and electrostatic interaction [36]. Furthermore, chemical pre-treating of adsorbents can increase their surface-active protons, and thereby their chemisorption capability [27, 36, 37]. In the Lu et al. study, CNTs were synthesized by catalytic chemical vapor deposition method, and then by HCl, H_2SO_4, HNO_3, and NaOCl solutions, separately. The NaOCl-oxidized CNTs had superior adsorption performance of BTEX from the aqueous solution compared to the untreated activated carbon [18]. Therefore, the 30% NaOCl solution and 10 s ultrasonication time were selected as the optimum conditions for adsorbent modification.

The effect of pH

The results of the ATN adsorption on M-MWCNTs in various pHs showed that this parameter plays an effective role in the

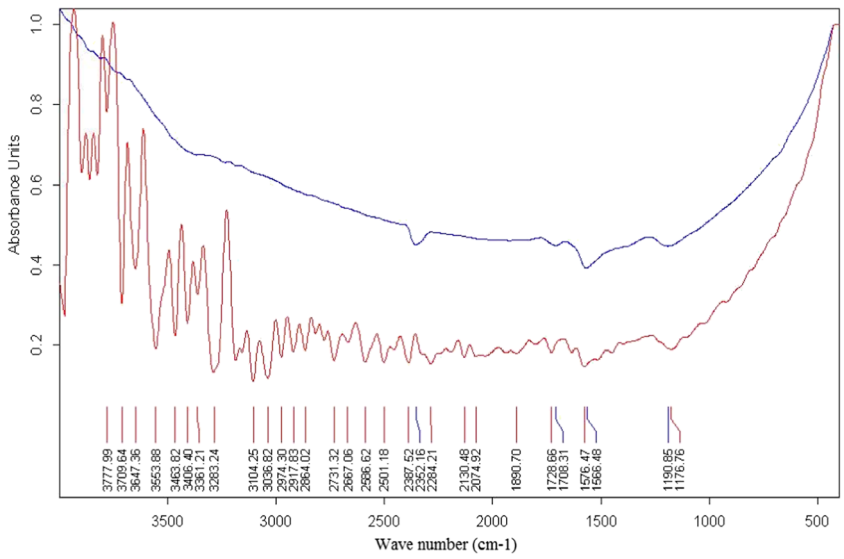

Fig. 5 FT-IR spectra of untreated MWCNTs (red line) and M-MWCNTs (blue line)

Table 2 ATN removal on untreated MWCNTs and MWCNTs treated in different Conditions (Ultrasonic wave frequency: 22 kHz, contact time with NaOCl solution: 2 h)

solution	Concentration (%)	Ultrasonication time (sec)	Removal (%)
NaOCl	60	1	55.89
		5	59.38
		10	76.14
		20	78.11
	30	1	59.87
		5	64.63
		10	87.89
		20	83.21
Distilled water	–	1	45.13
		5	56.14
		10	58.63
		20	58.72
Untreated MWCNTs			58.2

adsorption process (Fig. 6). According to the experimental study, the ATN adsorption rate at pH less and more than 6, the removal efficiency was reduced, and from pH 6 to 9, this reduction continued, however, re-increased at pHs more than 9. Therefore, the highest ATN removal rate was observed at pH = 6 with a yield of 86.08%. In acidic pH close to 6, the carboxyl and hydroxyl functional groups are protonated on the surface of CNTs and the adsorbent surface has a positive charge, which promotes the total adsorption through the electrostatic interaction between the adsorbent and the adsorbate. However, in pHs greater than 6, the amount of ATN removal

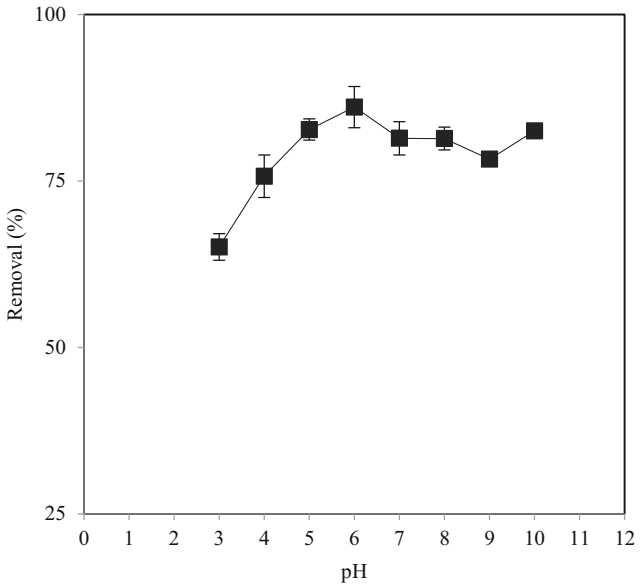

Fig. 6 Effect of pH on the ATN adsorption (ATN initial concentration of 5 mg L-1, room temperature, and contact time of 120 min)

was reduced due to an increase in negative charge and electrostatic repellence between adsorbent and adsorbate [1]. In addition, at higher pHs of 9, the competition of OH^- ion with ATN for occupation activated sites is another factor reducing the efficiency of ATN elimination [15, 38]. The optimum pH of ATN adsorption on M-MWCNTs was lower than the pHzpc value (7.6, see supplementary material), meaning that the adsorbent surface was positively charged (attracting anions) and the acidic water donates more protons than hydroxide groups [39].

On the other hand, regarding ATN has an octanol-water partition coefficient (K_{ow}) of 0.23 and is a lipid insoluble hydrophilic compound ($pK_a = 9.6$) [40]; therefore, adsorption seems to be a suitable process for removing it from aqueous solutions.

In the current study, it was found that the oxidation of carbon nanotubes by various chemical solutions leads to the formation of different functional groups on them, so that the total acidity of the carbon nanotubes has increased after the oxidation, which can be due to the presence of phenol, lactone, and carboxyl groups. The main factors of acidity were respectively carboxylic groups followed by lactone and phenolic groups [18].

In the study of Haro, et al. [7] the optimum pH value equal to 6 was found for the removal of ATN by granular activated carbon. The optimum pH of 7 was obtained in the study of Ardakani and Zandipak [41] about Janus Green dye removal onto MWCNTs. While, the most effective removal of amoxicillin by commercial activated carbon and NH_4Cl-induced activated carbon was reported at pH 6 [42].

Effect of contact time and kinetic modeling

The kinetic of ATN adsorption on M-MWCNTs was investigated over a 150-min period at initial concentration of 5 mg L^{-1} and the optimized pH of 6. The ATN adsorption rate during the early minutes of experiments was much higher than the late one, in other words, the adsorption capacity of adsorbate increases during the early minutes (Fig. 7). This may be attributed to the presence of specific functional groups and abundant unsaturated active sites on the outer surfaces of M-MWCNTs at the beginning phase of adsorption [1, 43]. Moreover, the incremental adsorption of ATN in the early minutes showed that M-MWCNTs had a high ability to remove ATN over a short period of time, which was very important in terms of energy and cost saving. After 90 min, almost no significant changes in the ATN adsorption capacity were observed, so 90 min was considered as the equilibrium time in the next adsorption experiments. Our results are compatible with those of similar studied e.g. Naghizadeh et al. who obtained the maximum RB-29 adsorption capacity (q_m) of chitin onto shrimp shell as 116.07 mg g^{-1} at 50 mg L^{-1} and contact time of 90 min [44].

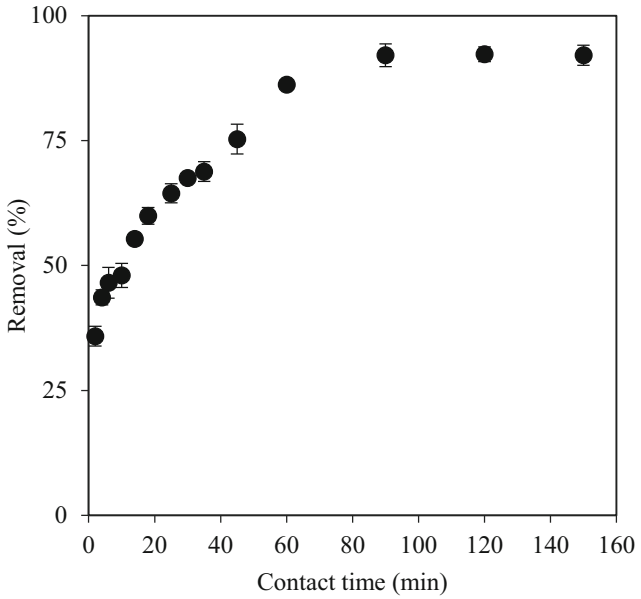

Fig. 7 Effect of contact time on ATN adsorption onto M-MWCNTs (ATN initial concentration of 5 mg L^{-1}, room temperature, and pH of 6)

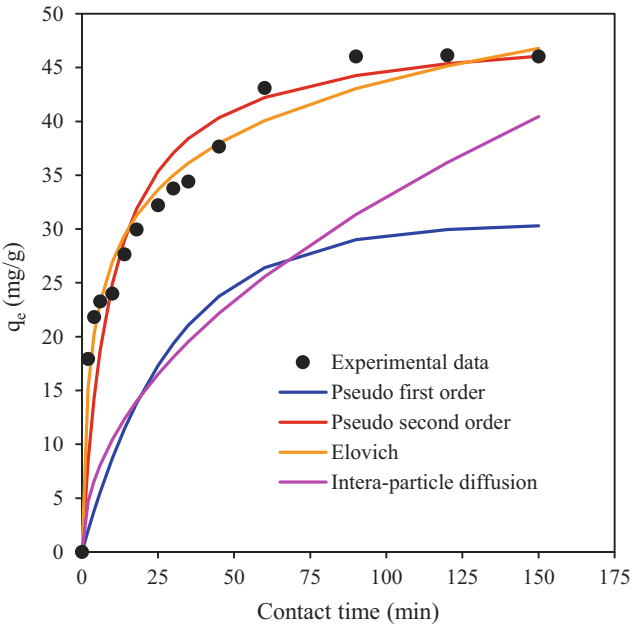

Fig. 8 Kinetic model plots for ATN adsorption onto M-MWCNTs

According to a previous study Pourzamani et al., the highest removal efficiency of benzene removal from aqueous solution by MWCNTs was observed at 20 min and there was a direct correlation between removal efficiency and contact time [19]. Further, in another study, the optimum time of 75 min was obtained to remove dye by CNTs [41]. In a similar research, the best results were found after 90 min to adsorb ATN onto granular activated carbon [7], which is similar to equilibrium time obtained in the current study. In the study of ATN elimination by cherry seed, the best equilibrium time was obtained at 60 min, then, by an increase of the contact time, a decreasing trend was observed. The reason was attributed to the presence of negative charges on the surface of adsorbent after equilibrium time [45]. In general, by increasing the contact time, availability of the adsorbate ions to unoccupied active sites on the adsorbent surface decreases and ultimately these sites become saturated when the process reaches the equilibrium point [8].

In our study, four well-known models, including pseudo first order, pseudo second order, intra-particle diffusion, and Elovich were used to describe the adsorption process kinetic (Fig. 8). The kinetic parameter values of ATN adsorption onto M-MWCNTs have been presented in Table 3. As seen, the R^2 values of pseudo first order, pseudo second order, Elovich and intra-particle diffusion were 0.943, 0.994, 0.958, and 0.863, respectively. The values of X^2 and NSD of pseudo first order were higher than those of pseudo second order and Elovich.

Low correlation coefficient (0.863), higher values of X^2 (10.95) and NSD (3385.9), as well as K_i value higher than zero, representing the thickness of boundary layer, demonstrate that the intra-particle diffusion model was not the only controlling step of the process. It reveals that adsorption of ATN on the M-MWCNTs was a multi-step process, involving the adsorption on the external surface and diffusion into the interior.

Table 3 also shows that the calculated capacity of the pseudo second order model ($q_{e,cal} = 49.01$ mg g^{-1}) was closer to its experimental value ($q_{e,exp} = 46.03$ mg g^{-1}). These explanations verify that the adsorption of ATN on M-MWCNTs was better fitted by pseudo second order models; expressing chemisorption was the dominant mechanism controlling the process of ATN adsorption on M-MWCNTs. This also means that the ion exchanging or electrons sharing had been occurred between adsorbate and the binding sites on the M-MWCNTs [24, 28]. Chemisorption process is typically limited to one layer of molecules on the surface of the adsorbent commonly followed by added layers of the physically adsorbed molecules of the adsorbate [46, 47].

The pseudo second order model also indicates that two parallel reactions are involved in the ATN adsorption on M-MWCNTs; the first one that quickly arrives to equilibrium and the second slower one that last longer [26, 27]. Haro, et al. [7] evaluated ATN adsorption on the activated carbon and reported the pseudo second order as the suitable kinetic model for data description.

Isotherm modeling

Equilibrium data commonly known as adsorption isotherms provide basic requirements for the design of adsorption systems. These data express the capacity of the adsorbent or the amount required to remove a unit mass of the pollutant under the system conditions [24]. In order to evaluate the ATN adsorption equilibrium on

Table 3 Kinetic models parameters for the adsorption of ATN by M-MWCNTs (pH of 6, ATN initial concentration of 5 mg L^{-1}, and room temperature)

Kinetic models	Constants				
Pseudo first order	$q_{e,\ Cal}$ (mg g^{-1})	K_1 (min^{-1})	R^2	X^2	NSD
	30.49	0.0335	0.943	14.55	3390.8
Pseudo second order	$q_{e,\ Cal}$ (mg g^{-1})	K_2 (g mg^{-1} min^{-1})	R^2	X^2	NSD
	49.01	0.0021	0.994	0.4864	3346.5
Elovich	α	β	R^2	X^2	NSD
	0.5437	7.3176	0.958	0.1076	3344.9
Intra-particle diffusion	K_i		R^2	X^2	NSD
	3.3029		0.863	10.95	3385.9
Experimental	$q_{e,\ exp}$ (mg g^{-1})				
	46.03				

M-MWCNTs and the mechanisms affecting it, three isotherm models, including Langmuir, Freundlich, and Temkin were selected. The results of the adsorption isotherm parameters for different equations are presented in Table 4. According to R^2, X^2, and NSD values, the ATN adsorption behavior on M-MWCNTs followed from both Freundlich (0.97) and Langmuir (0.95) models, although the adsorption process somewhat fits more with the Freundlich model. Temkin isotherm was also tested in the investigation.

The R^2 of Temkin model was roughly comparable with the Langmuir and Freundlich R^2, which highlighted the extent to which the Temkin model is applicable for the adsorption of ATN by M-MWCNTs. The process fitness according to Langmuir adsorption model describes monolayer and homogeneous adsorption of adsorbate on the surface while the Freundlich model suggests the adsorption is occurred onto a multilayer and heterogeneous surface [27].

Once again in Table 4, the n value in the Freundlich model was higher than 2 (between 2 to 10), indicating the favorable adsorption of ATN onto M-MWCNTs. Furthermore, in the Langmuir model, the value of R_L was between 0 and 1, which represents that ATN molecules were favorably adsorbed by the adsorbent [26].

Moreover, the maximum ATN adsorption capacity (q_m) of M-MWCNTs based on the Langmuir model was equal to 61.72 mg g^{-1}, indicating the good capacity of M-MWCNTs in removal of pharmaceutical pollutants existed in wastewaters. The q_m of current adsorbent is comparable to similar materials used to pharmaceutical pollutant removal [8, 38, 48]. The constant values of Langmuir (K_L) and Freundlich (K_F) were 1.29 L mg^{-1} and 33.72 (mg g^{-1}) (l mg^{-1}) n^{-1}, respectively. Considering that the larger values of the two constants indicate that the adsorption is more favorable [26], it is concluded that the M-MWCNTs have a good adsorption capacity for ATN removal as compared to carbons in the same researches [1, 8].

Table 4 Isotherm parameters of ATN adsorption on M-MWCNTs for different equations (pH of 6, contact time of 90 min, ATN initial concentration of 5 mg L^{-1}, and room temperature)

		Coefficient/constant					
Isotherm model	Langmuir	q_m (mg g^{-1})	K_L (l mg^{-1})	R_L	R^2	X^2	NSD
		61.72	1.29	0.67	0.95	0.189	2330.8
	Freundlich	n	k_f (mg g^{-1})(l mg^{-1}) $^{n-1}$		R^2	X^2	NSD
		2.60	33.72		0.97	0.064	2330.5
	Temkin	K_T	B_T		R^2	X^2	NSD
		13.85	13.85		0.93	0.13	2330.5

Thermodynamic study

The increasing temperature can have two major effects on the adsorption process. First, it increases the diffusion rate of the adsorbate molecules into internal pores and the external boundary layer of adsorbent as a result of the reduced viscosity of the solution. Second, it amends the equilibrium capacity of the adsorbent for a specific adsorbate [47].

The ATN adsorption studies were carried out at different temperatures of 20, 30, 40, and 50 °C (Fig. 9). As seen, the adsorption capacity improves with the increasing temperature from 20 °C to 40 °C, indicating that adsorption is an endothermic process in this temperature range. This may be a result of the increase in the ATN mobility upon temperature rising. The growing number of molecules may also attain sufficient energy to undertake an interaction with active sites at the surface [25]. Furthermore, the increasing temperature may produce an enlarging effect within the internal structure of M-MWCNTs and cause the large ATN molecule to penetrate more [43]. However, with an additional increase in temperature to 50 °C, the ATN removal

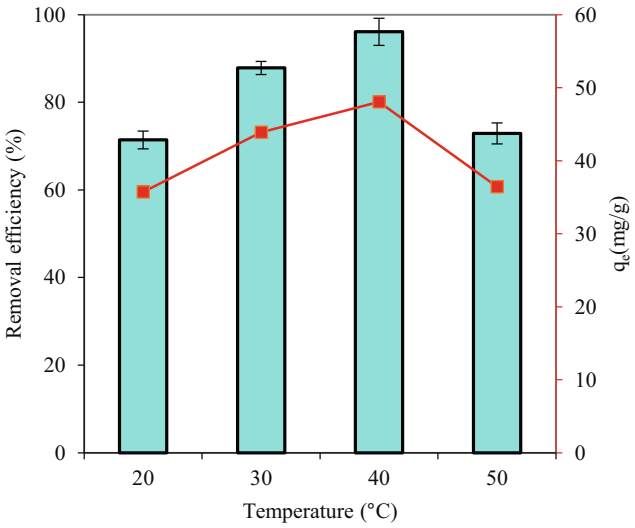

Fig. 9 Effect of different temperatures on ATN adsorption onto M-MWCNTs (ATN initial concentration of 5 mg L^{-1}, room temperature, pH of 6, and contact time of 90 min)

Table 5 Thermodynamic parameters of ATN adsorption on M-MWCNTs (pH of 6, contact time of 90 min, ATN initial concentration of 5 mg L^{-1})

Temperature (°K)	Parameters			
	Ln k_c	ΔG° (kJ mol^{-1})	ΔH° (kJ mol^{-1})	ΔS° (kJ mol^{-1} K^{-1})
293	5.54×10^4	-1.35×10^8		
303	5.73×10^4	-1.45×10^8	−1573.6	9.18
313	5.92×10^4	-1.54×10^8		
323	6.11×10^4	-1.64×10^8		

efficiency was reduced. This can be because high temperatures cause damage to the adsorbent structure.

The values of thermodynamic parameters such as (ΔG°), (ΔH°), and (ΔS°) for the adsorption of ATN on M-MWCNTs are shown in Table 5. The negative value of ΔH^o suggests that the adsorption process was exothermic and it was not favored at higher temperatures [39]. Moreover, the positive value of ΔS^o is an indicator of the ATN tendency toward the adsorbent, It also demonstrates the improved efficiency as a result of the increasing temperature in solid and liquid phases during the adsorption process. In other words, positive ΔS^o values imply that the degree of disorder increased during the adsorption process [25].

The negative values of ΔG° confirm that the process of ATN adsorption on M-MWCNTs is spontaneous and feasible. Since ΔH^o value of ATN adsorption is greater than 40 kJ mol^{-1}, it can be concluded that the adsorption process had a chemical mechanism [35].

ANN modeling

In the current study, initially, the ANN model with different back propagation algorithms was developed to estimate the performance of the ATN adsorption process. Among all back-propagation algorithms, the Levenberg–Marquardt algorithm typically resulted in a lower MSE, which was then selected as the training algorithm in the present study.

The optimal structure of ANN model achieved based on the minimum value of MSE and the maximum value of R^2 for testing set. Figure 10 shows four scatter plots, evaluating the experimental values against the predicted neural network values for all training, testing, and validating data. According to Fig. 10, approximately the whole values dispersed around the 45° line, indicating a good compatibility between the trial results and ANN-

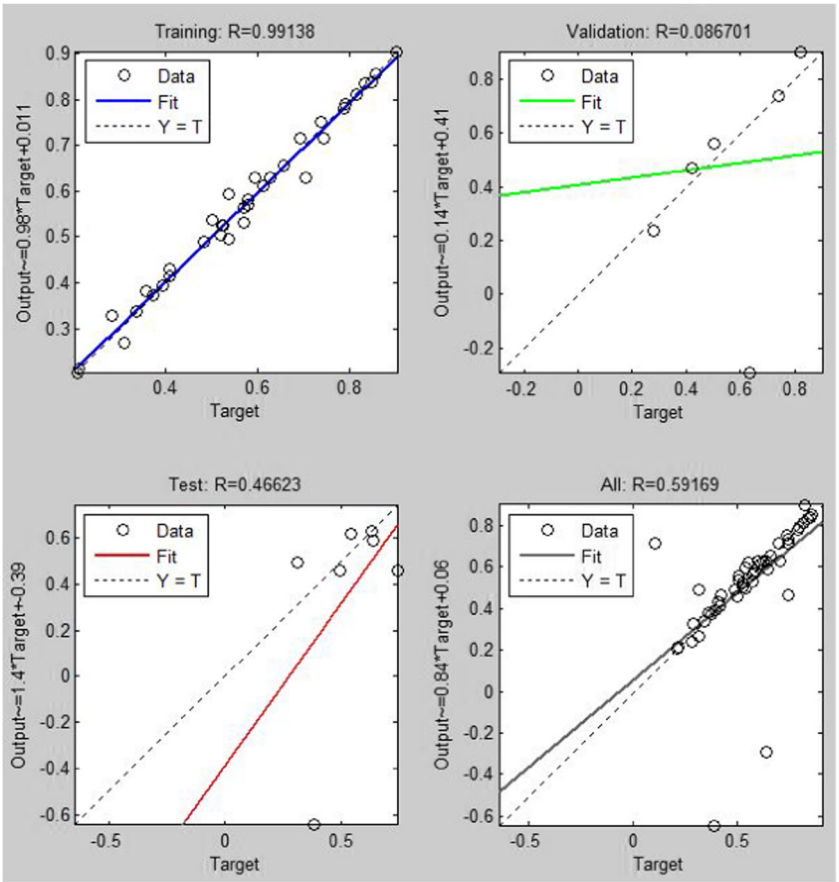

Fig. 10 ANN model results according to different divisions of datasets

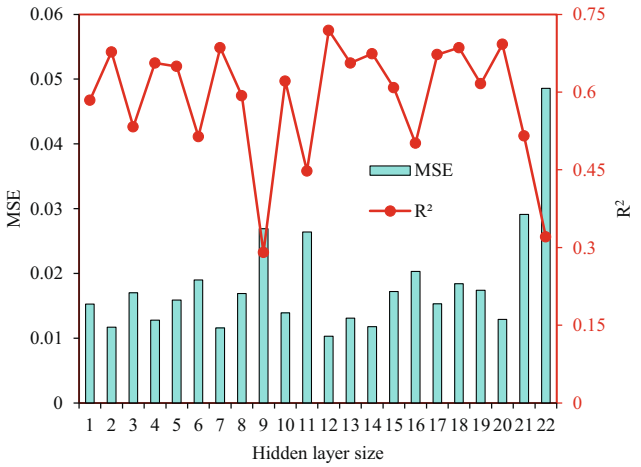

Fig. 11 The relation among number of neurons, R^2, and MSE for the ANN modeling of ATN adsorption onto M-MWCNTs

predicted data. Correspondingly, Fig. 11 presents the relation between the number of neurons, R^2, and MSE for the ANN modeling of ATN adsorption onto M-MWCNTs.

Figure 12 illustrates the relationship between the experimental and predicted values of ATN removal using the ANN model for the whole dataset after de-normalization. The determination coefficient (R^2) for training data was 0.9492 and for testing data was 0.9911. These results are in agreement with previous studies, which reported a determination coefficient of 0.9813 for microcystins LR adsorption using MWCNT-Fe_3O_4 [24] and 0.98 for adsorption of triamterene using multi-walled and single-walled carbon nanotubes [1].

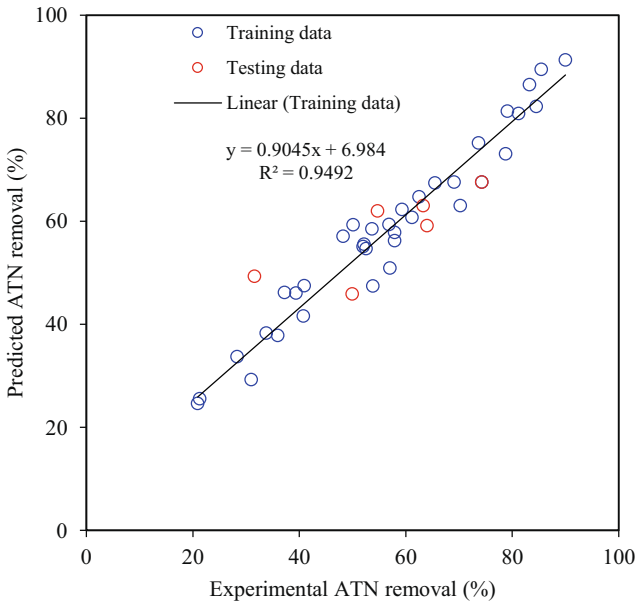

Fig. 12 Relationship between the experimental and predicted values of ATN removal onto M-MWCNTs

Conclusion

As one of the most frequently prescribed β-blocker drugs, ATN exists widely in hospitals and municipal wastewaters. In this study, we investigated the ability of MWCNTs modified by NaOCl and ultrasonic treatment in treating the aqueous environment containing ATN drug. The results of our study showed that the application of reasonable NaOCl concentration and ultrasonic frequency remove many impurities, increase porosity, and thereby significantly improves adsorption efficiency of MWCNTs. However, if the time and frequency of ultrasonic waves, as well as the chlorine concentration in the liquid exceed the optimal levels, these led to oxidizing the adsorbent context and ultimately reducing adsorption capabilities. The highest ATN removal occurred in the adsorbent activated within 10 s, but increasing the activation time to 20 s reduced the removal efficiency. Therefore, the adsorbent treatment with the proposed method of this study is not time consuming and also is not rather costly. Based on TGA, M-MWCNTs are stable without any significant loss from about 40 °C to 537.88 °C. Moreover, we proved that ANN can be a good way to estimate the experimental data in different conditions (more than 94% accuracy).

Acknowledgements Our deepest appreciations are expressed to the Isfahan University of Medical Sciences that supported this study financially.

Compliance with ethical standards

Conflict of interest The authors declare that they have no conflict of interest.

References

1. Ghaedi A, Ghaedi M, Pouranfard A, Ansari A, Avazzadeh Z, Vafaei A, et al. Adsorption of triamterene on multi-walled and single-walled carbon nanotubes: artificial neural network modeling and genetic algorithm optimization. J Mol Liq. 2016;216:654–65.
2. Samadi MT, Shokoohi R, Araghchian M, Tarlani AM. Amoxicillin removal from aquatic solutions using multi-walled carbon nanotubes. J Mazandaran Uni Med Sci. 2014;24(117):103–15.
3. Kyzas GZ, Koltsakidou A, Nanaki SG, Bikiaris DN, Lambropoulou DA. Removal of beta-blockers from aqueous media by adsorption onto graphene oxide. Sci Total Environ. 2015;537:411–20.
4. Divya K, Narayana B. New visible spectrophotometric methods for the determination of atenolol in pure and dosage forms via complex formation. Indo Am j pharm res. 2014;4(1):194–203.
5. Urtiaga A, Pérez G, Ibáñez R, Ortiz I. Removal of pharmaceuticals from a WWTP secondary effluent by ultrafiltration/reverse osmosis followed by electrochemical oxidation of the RO concentrate. Desalination. 2013;331:26–34.
6. Maszkowska J, Stolte S, Kumirska J, Łukaszewicz P, Mioduszewska K, Puckowski A, et al. Beta-blockers in the

environment: part I. Mobility and hydrolysis study. Sci Total Environ. 2014;493:1112–21.
7. Haro NK, Del Vecchio P, Marcilio NR, Féris LA. Removal of atenolol by adsorption–study of kinetics and equilibrium. J Clean Prod. 2017;154:214–9.
8. Hu Y, Fitzgerald NM, Lv G, Xing X, Jiang W-T, Li Z. Adsorption of atenolol on kaolinite. Adv Mater Sci Eng. 2015;2015:1–8.
9. Papageorgiou M, Kosma C, Lambropoulou D. Seasonal occurrence, removal, mass loading and environmental risk assessment of 55 pharmaceuticals and personal care products in a municipal wastewater treatment plant in Central Greece. Sci Total Environ. 2016;543:547–69.
10. Isarain-Chávez E, Rodríguez RM, Cabot PL, Centellas F, Arias C, Garrido JA, et al. Degradation of pharmaceutical beta-blockers by electrochemical advanced oxidation processes using a flow plant with a solar compound parabolic collector. Water Res. 2011;45(14):4119–30.
11. Klavarioti M, Mantzavinos D, Kassinos D. Removal of residual pharmaceuticals from aqueous systems by advanced oxidation processes. Environ Int. 2009;35(2):402–17.
12. Wilde ML, Montipó S, Martins AF. Degradation of β-blockers in hospital wastewater by means of ozonation and Fe 2+/ozonation. Water Res. 2014;48:280–95.
13. Arola K, Hatakka H, Mänttäri M, Kallioinen M. Novel process concept alternatives for improved removal of micropollutants in wastewater treatment. Sep Purif Technol. 2017.
14. Gholizadeh A, Ebrahimi AA, Salmani MH, Ehrampoush MH. Ozone-cathode microbial desalination cell; an innovative option to bioelectricity generation and water desalination. Chemosphere. 2017;188:470–7. https://doi.org/10.1016/j.chemosphere.2017.09.009.
15. Sotelo J, Rodríguez A, Álvarez S, García J. Modeling and elimination of atenolol on granular activated carbon in fixed bed column. Int J Environ Res. 2012;6(4):961–8.
16. Awual MR, Khraisheh M, Alharthi NH, Luqman M, Islam A, Karim MR, et al. Efficient detection and adsorption of cadmium (II) ions using innovative nano-composite materials. Chem Eng J. 2018;343:118–27.
17. Rahmani A, Mousavi HZ, Fazli M. Effect of nanostructure alumina on adsorption of heavy metals. Desalination. 2010;253(1):94–100.
18. Lu C, Su F, Hu S. Surface modification of carbon nanotubes for enhancing BTEX adsorption from aqueous solutions. Appl Surf Sci. 2008;254(21):7035–41.
19. Pourzamani H, Hajizadeh Y, Fadaei S. Efficiency enhancement of multi-walled carbon nanotubes by ozone for benzene removal from aqueous solution. Int J Environ Health Eng. 2015;4(1):29.
20. Lee C-G, Lee S, Park J-A, Park C, Lee SJ, Kim S-B, et al. Removal of copper, nickel and chromium mixtures from metal plating wastewater by adsorption with modified carbon foam. Chemosphere. 2017;166:203–11.
21. Gholizadeh A, Kermani M, Gholami M, Farzadkia M, Yaghmaeian K. Removal efficiency, adsorption kinetics and isotherms of phenolic compounds from aqueous solution using Rice bran ash. Asian J Chem. 2013;25(7):3871–8.
22. Naghizadeh A, Momeni F, Derakhshani E. Efficiency of ultrasonic process in regeneration of graphene nanoparticles saturated with humic acid. Desalin Water Treat. 2017;70(2017):290–3.
23. Nyairo WN, Eker YR, Kowenje C, Akin I, Bingol H, Tor A, et al. Efficient adsorption of lead (II) and copper (II) from aqueous phase using oxidized multiwalled carbon nanotubes/polypyrrole composite. Sep Sci Technol. 2018;53(10):1498–510.
24. Baziar M, Azari A, Karimaei M, Gupta VK, Agarwal S, Sharafi K, et al. MWCNT-Fe3O4 as a superior adsorbent for microcystins LR removal: Investigation on the magnetic adsorption separation, artificial neural network modeling, and genetic algorithm optimization. J Mol Liq. 2017;241(Supplement C):102–13. https://doi.org/10.1016/j.molliq.2017.06.014.
25. Ceylan Z, Mustafaoglu D, Malkoc E. Adsorption of phenol by MMT-CTAB and WPT-CTAB: equilibrium, kinetic and thermodynamic study. Particulate Sci Technol. 2018:36(6).
26. Behnamfard A, Salarirad MM. Equilibrium and kinetic studies on free cyanide adsorption from aqueous solution by activated carbon. J Hazard Mater. 2009;170(1):127–33.
27. Gholizadeh A, Kermani M, Gholami M, Farzadkia M. Kinetic and isotherm studies of adsorption and biosorption processes in the removal of phenolic compounds from aqueous solutions: Comparative study. J Environ Health Sci Eng. 2013;11(1). https://doi.org/10.1186/2052-336X-11-29.
28. Ben-Ali S, Jaouali I, Souissi-Najar S, Ouederni A. Characterization and adsorption capacity of raw pomegranate peel biosorbent for copper removal. J Clean Prod. 2017;142(Part 4):3809–21. https://doi.org/10.1016/j.jclepro.2016.10.081.
29. Choi S, Gray ML, Jones CW. Amine-tethered solid adsorbents coupling high adsorption capacity and regenerability for CO2 capture from ambient air. ChemSusChem. 2011;4(5):628–35.
30. Vairavapandian D, Vichchulada P, Lay MD. Preparation and modification of carbon nanotubes: review of recent advances and applications in catalysis and sensing. Anal Chim Acta. 2008;626(2):119–29.
31. Zhang Z, Wu G, Xu Z, Wu S, Gu L. Adsorption of Methyl Blue onto uniform carbonaceous spheres prepared via an anionic polyacrylamide-assisted hydrothermal route. Mater Chem Phys. 2018.
32. Omastová M, Mičušík M, Fedorko P, Pionteck J, Kovářová J, Chehimi MM. The synergy of ultrasonic treatment and organic modifiers for tuning the surface chemistry and conductivity of multiwalled carbon nanotubes. Surf Interface Anal. 2014;46(10–11):940–4.
33. Dotto GL, Santos JMN, Rodrigues IL, Rosa R, Pavan FA, Lima EC. Adsorption of methylene blue by ultrasonic surface modified chitin. J Colloid Interface Sci. 2015;446:133–40. https://doi.org/10.1016/j.jcis.2015.01.046.
34. Su F, Lu C, Hu S. Adsorption of benzene, toluene, ethylbenzene and p-xylene by NaOCl-oxidized carbon nanotubes. Colloids Surf A Physicochem Eng Asp. 2010;353(1):83–91.
35. Chen Y-C, Lu C. Kinetics, thermodynamics and regeneration of molybdenum adsorption in aqueous solutions with NaOCl-oxidized multiwalled carbon nanotubes. J Ind Eng Chem. 2014;20(4):2521–7.
36. Yu F, Ma J, Wu Y. Adsorption of toluene, ethylbenzene and xylene isomers on multi-walled carbon nanotubes oxidized by different concentration of NaOCl. Frontiers of Environmental Science & Engineering. 2012;6(3):320–9. https://doi.org/10.1007/s11783-011-0340-4.
37. Alahabadi A, Rezai Z, Rahmani-Sani A, Rastegar A, Hosseini-Bandegharaei A, Gholizadeh A. Efficacy evaluation of NH4Cl-induced activated carbon inÂ removal of aniline from aqueous solutions and comparing its performance with commercial activated carbon. Desalin Water Treat. 2016;57(50):23779–89. https://doi.org/10.1080/19443994.2015.1134356.
38. Delgado LF, Charles P, Glucina K, Morlay C. Adsorption of ibuprofen and atenolol at trace concentration on activated carbon. Sep Sci Technol. 2015;50(10):1487–96.
39. Kakavandi B, Jonidi AJ, Rezaei RK, Nasseri S, Ameri A, Esrafily A. Synthesis and properties of Fe3O4-activated carbon magnetic nanoparticles for removal of aniline from aqueous solution: equilibrium, kinetic and thermodynamic studies. Iranian J Environ Health Sci Eng. 2013;10(1):19. https://doi.org/10.1186/1735-2746-10-19.
40. Karaman R. From Conventional Prodrugs to Prodrugs Designed By Molecular Orbital Methods. Frontiers in Computational Chemistry. Elsevier; 2015. p. 187–249.

41. Ardakani SS, Zandipak R. Evaluation of carbon nanotubes efficiency for removal of Janus green dye from Ganjnameh River water sample. J Health Dev. 2014;3(4):282–0.
42. Moussavi G, Alahabadi A, Yaghmaeian K, Eskandari M. Preparation, characterization and adsorption potential of the NH4Cl-induced activated carbon for the removal of amoxicillin antibiotic from water. Chem Eng J. 2013;217(Supplement C): 119–28. https://doi.org/10.1016/j.cej.2012.11.069.
43. Miraboutalebi SM, Nikouzad SK, Peydayesh M, Allahgholi N, Vafajoo L, McKay G. Methylene blue adsorption via maize silk powder: kinetic, equilibrium, thermodynamic studies and residual error analysis. Process Saf Environ Prot. 2017;106:191–202.
44. Naghizadeh A, Ghafouri M, Jafari A. Investigation of equilibrium, kinetics and thermodynamics of extracted chitin from shrimp shell in reactive blue 29 (RB-29) removal from aqueous solutions. Desalin Water Treat. 2017;70:355–63.
45. Ismael HA, Khdum LH, Lafta AJ. Use of Iraqi cherry seeds in the removal of paracetamol and atenolol medicines from their aqueous solutions. Int J Sci Res (IJSR). 2014;3(12):2290–5.
46. Moradi S, Sadrjavadi K, Farhadian N, Hosseinzadeh L, Shahlaei M. Easy synthesis, characterization and cell cytotoxicity of green nano carbon dots using hydrothermal carbonization of gum Tragacanth and chitosan bio-polymers for bioimaging. J Mol Liq. 2018;259: 284–90. https://doi.org/10.1016/j.molliq.2018.03.054.
47. Takdastan A, Kakavandi B, Azizi M, Golshan M. Efficient activation of peroxymonosulfate by using ferroferric oxide supported on carbon/UV/US system: A new approach into catalytic degradation of bisphenol A. Chem Eng J. 2018;331(Supplement C):729–43. https://doi.org/10.1016/j.cej.2017.09.021.
48. Feng Z, Odelius K, Rajarao GK, Hakkarainen M. Microwave carbonized cellulose for trace pharmaceutical adsorption. Chem Eng J. 2018;346:557–66.